HOKKAIDO UNIVERSITY

Title	Alterations of cellular physiology in Escherichia coli in response to oxidative phosphorylation impaired by defective F1-ATPase
Author(s)	Noda, Sakiko; Takezawa, Yuji; Mizutani, Tomohiko; Asakura, Tomoaki; Nishiumi, Eiichiro; Onoe, Kazunori; Wada, Masaru; Tomita, Fusao; Matsushita, Kazunobu; Yokota, Atsushi
Citation	Journal of Bacteriology, 188(19), 6869-6876 https://doi.org/10.1128/JB.00452-06
Issue Date	2006-10
Doc URL	http://hdl.handle.net/2115/17010
Rights	Copyright © 2006 American Society for Microbiology
Type	article (author version)
File Information	JB188-19.pdf

Instructions for use

Alterations of cellular physiology in *Escherichia coli* in response to oxidative phosphorylation impaired by defective F$_1$-ATPase

Sakiko Noda,[1] Yuji Takezawa,[2] Tomohiko Mizutani,[1] Tomoaki Asakura,[1] Eiichiro Nishiumi,[1] Kazunori Onoe,[1] Masaru Wada,[1] Fusao Tomita,[2] Kazunobu Matsushita[3] and Atsushi Yokota[1*]

Laboratory of Microbial Physiology,[1] and Laboratory of Applied Microbiology,[2] Research Faculty of Agriculture, Hokkaido University, Kita 9 Nishi 9, Kita-ku, Sapporo, Hokkaido 060-8589, Japan; Department of Biological Chemistry, Faculty of Agriculture, Yamaguchi University, 1677-1, Yoshida, Yamaguchi, Yamaguchi 753-8515, Japan[3]

*Corresponding author

Mailing address: Laboratory of Microbial Physiology, Division of Applied Bioscience, Research Faculty of Agriculture, Hokkaido University, Kita 9 Nishi 9, Kita-ku, Sapporo, Hokkaido 060-8589, Japan

Tel: +81-11-706-2501; Fax: +81-11-706-4961

E-mail: yokota@chem.agr.hokudai.ac.jp.

Running Title: Physiology of F$_1$-ATPase mutant of *E. coli*

1 Abstract

2 The physiological changes in an F_1-ATPase-defective mutant of *E. coli* W1485 growing

3 in a glucose-limited chemostat included a decreased growth yield (60%) and increased

4 specific rates of both glucose consumption (168%) and respiration (171%). Flux analysis

5 revealed that the mutant showed approximately twice as much flow in glycolysis but only

6 an 18% increase in the tricarboxylic acid (TCA) cycle, owing to the excretion of acetate,

7 where most of the increased glycolytic flux was directed. Genetic and biochemical

8 analyses of the mutant revealed the downregulation of many TCA cycle enzymes,

9 including citrate synthase, and the upregulation of the pyruvate dehydrogenase complex

10 in both transcription and enzyme activities. These changes seemed to contribute to acetate

11 excretion in the mutant. No transcriptional changes were observed in the glycolytic

12 enzymes, despite the enhanced glycolysis. The most significant alterations were found in

13 the respiratory chain components. The total activity of NADH dehydrogenases (NDHs)

14 and terminal oxidases increased about twofold in the mutant, which accounted for its

15 higher respiration rate. These changes primarily arose from the increased (3.7-fold)

16 enzyme activity of NDH-2 and an increased amount of cytochrome *bd* in the mutant.

17 Transcriptional upregulation appeared to be involved in these phenomena. As NDH-2

18 cannot generate an electrochemical gradient of protons and as cytochrome *bd* is inferior

19 to cytochrome bo_3 in this ability, the mutant was able to recycle NADH at a higher rate

20 than the parent and avoid generating an excess proton-motive force. We discuss the

21 physiological benefits of the alterations in the mutant.

22

1 INTRODUCTION

2

3   The elucidation of the regulatory mechanism of glycolytic flux is critical for

4 developing effective fermentation processes for the production of useful metabolites by

5 microorganisms. Glycolytic flux in *Escherichia coli* is controlled primarily by the ATP

6 demand of the cells, rather than by glycolytic enzymes (22). For example, defects in the

7 activity of F_1F_o-ATP synthase that impair oxidative phosphorylation (21, 38, 40) or

8 increased ATPase activity in hydrolyzing ATP (22), which both lead to a reduced

9 [ATP]/[ADP] ratio (21, 22), result in enhanced rates of glucose consumption. The

10 enhancement of glucose consumption by defective F_1F_o-ATP synthase activity has also

11 been reported in the Gram-positive bacteria *Bacillus subtilis* (32) and *Corynebacterium*

12 *glutamicum* (34), which are industrially important. Several attempts have been made to

13 apply these findings to the production of useful metabolites from glucose by fermentation.

14 Our group reported the first successful application of pyruvate production, using an *E.*

15 *coli* mutant with a defective F_1-ATPase (40). In this case, enhanced pyruvate production

16 was achieved with an increased rate of glucose consumption. The effectiveness of

17 F_1F_o-ATP synthase defects for the production of acetate (9), as well as pyruvate (8), has

18 also been reported in different *E. coli* mutants. Recently we demonstrated that the

19 mutation also works for the improvement of glutamate production in *C. glutamicum* (1).

20   Although the [ATP]/[ADP] ratio is well accepted as a controlling factor of

21 glycolysis, the underlying mechanisms by which enhanced glucose metabolism is

22 established in response to an energy shortage are still not well understood. The allosteric

23 activation of the key enzymes in the glycolytic pathway, *i.e.*, phosphofructokinase I (2)

1 and pyruvate kinase II (23), under a reduced [ATP]/[ADP] ratio is thought to contribute to

2 this phenomenon. However, previous works (21, 38) have suggested the possibility that

3 qualitative changes in certain cell components, such as an increase in *b*-type cytochrome

4 contents, as well as allosteric control, are involved in the mechanism of enhanced glucose

5 metabolism. To address this important question, we investigated the alterations in cellular

6 physiology that occur in *E. coli* in response to impaired oxidative phosphorylation due to

7 a defective F_1-ATPase. To avoid any metabolic distortion from unnecessary genetic

8 background, we constructed a simple F_1-ATPase-defective mutant from the wild-type *E.*

9 *coli* W1485. Glucose-limited chemostat culture was employed to ensure that cell samples

10 grew at the same rate in the exponential phase. We conducted detailed analyses of

11 metabolic flux, gene expression profiles, and central carbon metabolic and respiratory

12 chain enzyme activities to elucidate the mechanism(s) of enhanced glucose metabolism.

13

14 **MATERIALS AND METHODS**

15

16   **Bacterial strains and culture conditions**. The wild-type strain *E. coli* W1485

17 (ATCC12435) was used. An F_1-ATPase-defective mutant, HBA-1 (*atpA401*, *bgl$^+$*), was

18 constructed by the P1kc transduction of *atpA401* (4), a defective gene for the α subunit of

19 F_1-ATPase, into strain W1485. This mutant allele was first isolated in 1971 by Butlin et

20 al., (4) as a gene (*uncA401*) that causes uncoupling of phosphorylation associated with

21 electron transport. The *E. coli* K12 strain carrying *uncA401* showed negligible activity of

22 Ca^{2+}, Mg^{2+}-activated ATPase (4). A series of intensive investigations of this mutant allele

23 has located this mutation in the α subunit of F_1-ATPase (13) and the sequence analysis

1 has revealed a single base change that resulted in the replacement of Ser 373 into Phe (29).

2 This mutant F_1-ATPase has been shown to have virtually no ATPase activity yet retain the

3 same subunits (α, β, γ, δ and ε) organization in terms of molecular weight, stoichiometry

4 ($\alpha_3\beta_3\gamma\delta\varepsilon$) and arrangement (6). This mutant F_1-ATPase has been suggested to bind to

5 ATPase-depleted membranes and keep proton impermeability of the membrane (6). This

6 was further confirmed in our preliminary experiment in which similar levels of

7 valinomycin-induced artificial membrane potential were monitored using inside-out

8 membrane vesicles prepared from strains W1485 and HBA-1 as monitored by

9 fluorescence quenching method (probe: bis-(1,3-dibutylbarbituric acid)pentamethine

10 oxonol (DiBAC$_4$(5)) (data not shown). Therefore, the membrane of the strain HBA-1 has

11 also been confirmed to be sealed and maintain normal level of proton impermeability. To

12 obtain transductants effectively, *atpA401* was co-transduced with *bgl$^+$*, as described

13 previously, using AN718bgl-7 as the donor strain (40). Almost no ATPase activity was

14 detected in strain HBA-1, when enzyme activity was measured as described previously

15 (40). Both strains were cultured in a glucose-limited chemostat in modified M9 minimal

16 medium containing trace elements to stabilize the continuous culture. The medium

17 contained 14.7 g/l $Na_2HPO_4 \cdot 12H_2O$, 3.0 g/l KH_2PO_4, 0.5 g/l NaCl, 1.0 g/l NH_4Cl, 1.0

18 mM $MgSO_4$, 0.1 mM $CaCl_2$, 1.0 μM $FeCl_3$, 0.03 μM $(NH_4)_6Mo_7O_{24}$, 4 μM H_3BO_3, 0.3

19 μM $CoCl_2$, 0. 1 μM $CuSO_4$, 0.8 μM $MnCl_2$, 0.1 μM $ZnSO_4$, and 2 g/l glucose as a carbon

20 source. The continuous chemostat culture was conducted at a dilution rate of 0.2 h^{-1}, with

21 a working volume of 750 ml, in a 2-L jar fermentor. The cultures were aerated at 1.5 l/min

22 (2 vvm), with stirring at 700 rpm. Dissolved oxygen (DO) in the culture broth of both

23 parent and mutant was monitored by a DO electrode and was maintained at about 90%.

1 The culture temperature was controlled at 37°C, and the pH was adjusted to 7.0 with

2 NaOH.

3 **Fermentation analysis.** Growth was measured by the spectrophotometric

4 absorbance of the culture broth at 660 nm. The concentration of glucose remaining in the

5 culture broth was determined by the glucose oxidase method, using Glucose C2 (Wako

6 Pure Chemical Industries, Ltd., Osaka, Japan). Organic acids in the culture broth were

7 determined by HPLC (column: AMINEX HPX-87H, Bio-Rad Laboratories, Hercules,

8 CA, USA; mobile phase: 0.01 N H_2SO_4; flow rate: 0.6 ml/min; detection: absorbance at

9 210 nm). The respiration rate of the bacterial cells during chemostatic culture was

10 measured using a dissolved oxygen analyzer (Model MD-1000, Iijima Electronics

11 Corporation, Gamagori, Aichi, Japan) equipped with a Clark-type oxygen electrode.

12 Measurements were conducted at 37°C in the air-tight chamber within the range yielding

13 a linear relationship between the cell concentration and the oxygen-consumption rate.

14 Our calculation assumed the oxygen solubility in the 37°C medium to be 0.214 mM. The

15 results were expressed as mmol O_2 h^{-1} (g dry cell weight)$^{-1}$. The dry cell weight of strains

16 W1485 and HBA-1 was determined from the correspondence of one optical density unit

17 at 660 nm to 0.414 mg and 0.411 mg dry cell weight per ml, respectively.

18 **Flux analysis.** The metabolic fluxes of the wild type strain and the mutant were

19 estimated using the stochiometric approach described by Holms (18). This method

20 provides the way to calculate metabolic fluxes within the central metabolic pathways in *E.*

21 *coli* growing on various single carbon sources at a constant growth rate. The idea is to

22 balance the metabolic events in the conversion of feedstock (glucose) to biomass and

23 by-products using the defined metabolic pathways and the experimental data of growth

1 rate, glucose consumption, by-product formation and biomass production. The kinetic

2 parameters (specific rates of glucose consumption and metabolites production) in

3 chemostat culture and the amounts of precursor metabolites required for the biosynthesis

4 of building blocks (27) were used to calculate the fluxes in the central metabolic

5 pathways.

6   **Extraction of total RNA.** Cells in the chemostat culture were withdrawn and

7 immediately mixed with crushed ice prepared at –80°C. The mixtures were centrifuged at

8 8,000 x g at 4°C for 10 min, and the supernatants were discarded. The RNA was isolated

9 from the cell pellet with ISOGEN (Nippon Gene Co., Ltd., Toyama, Tomaya, Japan),

10 according to the manufacturer's instructions. The RNA was treated with RQ1 RNase-Free

11 DNase (Promega Corporation, Madison, WI, USA) and extracted again with ISOGEN.

12 The concentration and quality of the total RNA yield were determined

13 spectrophotometrically and by agarose gel electrophoresis. The extracted RNA was kept

14 at –80°C until used.

15   **DNA array analysis.** For *E. coli*-specific primed cDNA synthesis, 2 μg total

16 RNA and 4 μl *E. coli* cDNA labeling primers (Sigma-Aldrich Corporation, St. Louis, MO,

17 USA) were added to the transcription mixture (6 μl 5x first-strand buffer and 1 μl each of

18 10 mM dATP, 10 mM dGTP, and 10 mM dTTP), and the total volume was adjusted to

19 26.5 μl with RNase-free water. The samples were incubated at 90°C for 2 min and were

20 kept at 42°C for 20 min. Then, 0.5 μl RNase inhibitor (20 U RNase OUT, Invitrogen

21 Corporation, Carlsbad, CA, USA), 1 μl reverse transcriptase (200 U, SuperScript II,

22 Invitrogen) and 2 μl [α-^{33}P]dCTP (20 μCi; GE Healthcare Bio-Sciences Corp.,

23 Piscataway, NJ, USA) were added to the reaction mixture. After incubation at 42°C for

1 2.5 h, the labeled cDNA was purified on a Sephadex G-25 spin column (GE Healthcare

2 Bio-Sciences). The purified cDNA was denatured at 94°C for 10 min and immediately

3 chilled on ice. The cDNA probe thus prepared was used to perform the hybridization

4 experiment using Panorama *E. coli* Gene Arrays (Sigma-Aldrich) as described in the

5 manufacturer's instructions. After hybridization, the arrays were exposed to Imaging

6 Plates (Fuji Photo Film Co., Ltd., Minami-Ashigara, Kanagawa, Japan) for 48 h. The

7 exposed Imaging Plates were scanned with BAS-5000 (Fuji Photo Film). Data analysis

8 was performed with Array Gauge software (v 1.2; Fuji Photo Film). The data were

9 calculated as the average and standard deviation of eight independent experiments and

10 expressed as a fraction of the total hybridization signal on each DNA array filter. A

11 two-tailed Student's *t*-test *p* value < 0.05 was considered statistically significant.

12 **Northern blot analysis.** The extracted total RNA was separated by

13 formaldehyde-agarose gel electrophoresis (9% formaldehyde, 1x MOPS buffer, pH 5.0, 5

14 mM sodium acetate, 1 mM EDTA, 1% agarose). The separated RNA was transferred onto

15 a Hybond-N$^+$ membrane (GE Healthcare Bio-Sciences) by the capillary method. To

16 detect *hns* gene expression with the hybridization probe, a 0.41-kb DNA fragment was

17 amplified by PCR using the following primer set: 5'-CGAAGCACTTAAAATTCTGA-3'

18 and 5'-TTATTGCTTGATCAGGAAAT-3'. Northern hybridization was carried out using

19 AlkPhos Direct and ECF substrate (GE Healthcare Bio-Sciences). The signals were

20 quantified by Typhoon 8600 (GE Healthcare Bio-Sciences) and ImageQuant software (v

21 5.2; Molecular Dynamics, Sunnyvale, CA, USA).

22 **Real-time PCR analysis.** The reaction mixture containing 5 μg total RNA, 1

23 μl random primers (300 ng, Invitrogen), and 1 μl 10 mM dNTP mixture in a total volume

1   of 12 μl was incubated at 65°C for 5 min and immediately chilled on ice. Then, 4 μl of 5x

2   first-strand buffer, 2 μl 0.1 M dithiothreitol (DTT) and 1 μl RNase inhibitor (40 U RNase

3   OUT, Invitrogen) were added, and the mixture was incubated at 25°C for 10 min and then

4   at 42°C for 2 min. After that, 1 μl reverse transcriptase (200 U; SuperScript II, Invitrogen)

5   was added, and the mixture was incubated at 42°C for 90 min, and then 70°C for 15 min.

6   The real-time PCR reaction was carried out in a 50-μl (total volume) mixture containing

7   25 μl 2x TaqMan Universal PCR Master Mix (Applied Biosystems, Foster City, CA,

8   USA), 900 nM each of forward and reverse primers, 200 nM TaqMan probe specific for

9   the target gene, and 5 μl of the cDNA sample. The amplification and detection of specific

10   products were performed with the ABI PRISM 7000 sequence detection system (Applied

11   Biosystems) using the following profile: incubation at 50°C for 2 min, 95°C for 10 min,

12   and 40 cycles at 95°C for 15 s and at 60°C for 1 min. Data analysis was performed using

13   the ABI PRISM 7000 sequence detection system software (v 1.0; Applied Biosystems).

14   Each sample was analyzed in duplicate. The sequences of the TaqMan probes and primers

15   for the target genes were as follows: *ndh* (Probe:

16   5'-FAM-CTGCTGCGGCCCACAACGAG-TAMRA-3'; Forward primer:

17   5'-TGCGTTACCGCCACGTATC-3'; Reverse primer:

18   5'-ACGCGAACGCCAAGTTTC-3'); *cyoA* (Probe:

19   5'-FAM-TTCCCGCAATCTTGATGGCT-TAMRA-3'; Forward primer:

20   5'-GGCCTGATGTTGATTGTCGTT-3'; Reverse primer:

21   5'-GGTACTTCCAGGCGAAACCA-3'); *cydA* (Probe:

22   5'-FAM-TTGCCTTGACCGCGATGTACCACTTC-TAMRA-3'; Forward primer:

23   5'-TCGAACTGTCGCGCTTACAG-3'; Reverse primer:

1 5'-CGAGCGTCAGTGGCACAA-3'). For the endogenous control, the 16S rRNA gene

2 *rrsA* was used (Probe: 5'-FAM-CCGGGCCTTGTACACACCGCC-TAMRA-3'; Forward

3 primer: 5'-GAATGCCACGGTGAATACGTT-3';   Reverse   primer:

4 5'-ACCCACTCCCATGGTGTGA-3'). A relative standard curve method was used to

5 calculate the relative expression level of the target gene. The expression ratio was

6 obtained by dividing the relative expression level of the mutant by that of the parent.

7   **Measurement of enzymes in central carbon metabolism.** Cells were

8 harvested by centrifugation, washed with an appropriate buffer, and kept at –20°C until

9 use. The cells were disrupted by sonication in the same buffer, and the cell debris was

10 removed by centrifugation at 39,000 x *g* at 4°C for 40 min. The supernatant was

11 gel-filtered using a PD-10 column (GE Healthcare Bio-Sciences) with the same buffer to

12 remove low-molecular-weight materials. The eluate was used as the crude enzyme for the

13 assay. The composition of the buffer system is described in the assay conditions of the

14 respective enzymes. Enzyme activity was monitored spectrophotometrically using a

15 Beckman DU 7400 spectrophotometer (Beckman Coulter, Inc., Fullerton, CA, USA) at

16 25°C. The protein concentration of the crude enzyme was determined using the Bio-Rad

17 Protein Assay (Bio-Rad Laboratories), with bovine serum albumin as the standard. The

18 specific activity of each enzyme under the assay conditions was expressed as nmole min^{-1}

19 (mg protein)$^{-1}$. For pyruvate dehydrogenase (PDH), 50 mM potassium phosphate buffer

20 (pH 8.1) was used as the washing and extraction buffer. The reaction mixture consisted of

21 50 mM potassium phosphate buffer (pH 8.1), 0.05 mM CoASH, 3 mM L-cysteine, 2.33

22 mM NAD$^+$, 0.2 mM thiamine pyrophosphate, 1 mM MgSO$_4$, 2 mM sodium pyruvate, and

23 the crude enzyme. The reaction was initiated by the addition of sodium pyruvate, and the

1   NADH concentration increase was monitored at 340 nm (39). For acetate kinase (ACK),

2   50 mM of imidazole-HCl buffer (pH 7.3) containing 10 mM $MgCl_2$ was used as the

3   washing and extraction buffer. The reaction mixture consisted of 50 mM imidazole-HCl

4   buffer (pH 7.3), 10 mM $MgCl_2$, 12 mM acetyl phosphate, 5 mM ADP, 10 mM glucose,

5   1.6 mM NADP, hexokinase (56 U/ml), and glucose 6-phosphate-dehydrogenase (1.5

6   U/ml). The reaction was initiated by the addition of ADP, and ATP formation was

7   monitored by the increase of the NADPH concentration at 340 nm (31). For citrate

8   synthase (CS), 20 mM Tris-HCl (pH 8.0) containing 10 mM $MgCl_2$ and 1 mM EDTA was

9   used as the washing and extraction buffer. Activity was measured in the reaction mixture,

10   which contained 100 mM Tris-HCl buffer (pH 8.0), 0.16 mM acetyl-CoA, 0.2 mM

11   oxaloacetic acid, and 0.1 mM 5,5'-dithiobis (2-nitrobenzoic acid) (DTNB). The reaction

12   was initiated by the addition of oxaloacetic acid. The CoA yield was monitored by the

13   absorbance increase at 412 nm. The molecular extinction coefficient of 13,600 M^{-1} cm^{-1}

14   for 5-mercapto-2-nitrobenzoic acid was used to calculate the enzyme activity (36). For

15   succinyl-CoA synthetase (SCS) (7), 20 mM potassium phosphate buffer (pH 7.2)

16   containing 20 mM $MgCl_2$ was used as the washing and extraction buffer. The reaction

17   mixture contained 50 mM Tris-HCl buffer (pH 7.2), 10 mM $MgCl_2$, 100 mM KCl, 10 mM

18   sodium succinate, 0.1 mM CoASH, and 0.4 mM ATP. The reaction was initiated by the

19   addition of ATP, and the formation of succinyl-CoA was monitored by the absorbance

20   increase at 230 nm. For succinyl-CoA, we used the molar extinction coefficient of 4900

21    $M^{-1}cm^{-1}$ at 230 nm to calculate enzyme activity. For malate dehydrogenase (MDH), 7 mM

22   potassium phosphate buffer (pH 7.0) containing 30% glycerol and 3.5 mM DTT was used

23   as the washing and extraction buffer. The reaction mixture consisted of 100 mM

1   potassium phosphate buffer (pH 7.2), 0.13 mM NADH, and 0.33 mM oxaloacetic acid.

2   The reaction was initiated by the addition of oxaloacetic acid. The decrease of NADH,

3   coupled with the formation of malate, was monitored at 340 nm (26).

4   **Measurement of enzymes in the respiratory chain.** Cells were washed with

5   50 mM potassium phosphate buffer (pH 7.5) containing 5 mM $MgSO_4$, 1 mM DTT, and

6   10% glycerol, resuspended in the same buffer, and then disrupted twice using a French

7   pressure cell (Ohtake Works, Tokyo, Japan) at 16,000 psi. The mixtures were centrifuged

8   at 8,000 x g at 4°C for 10 min, and the supernatant was ultracentrifuged at 120,000 x g, at

9   0°C for 2 h. The membrane fraction was suspended by homogenization with a

10   teflon-coated homogenizer in the same buffer and used as the crude enzyme for the

11   NADH dehydrogenase (NDH) assay. The activities of the NDHs were measured by

12   monitoring the decrease of the NADH or deamino-NADH concentration at 340 nm. The

13   reaction mixture consisted of 50 mM potassium phosphate buffer (pH 7.5), 5 mM $MgSO_4$,

14   and 0.125 mM of either NADH or deamino-NADH substrate. The reaction was initiated

15   by the addition of the crude enzyme. As deamino-NADH is the substrate for NDH-1 but

16   not for NDH-2 (25), the NDH-2 activity was calculated by subtracting the

17   deamino-NADH oxidase activity (NDH-1 activity) from the NADH oxidase activity

18   (total NDH activity). The protein concentration of the crude enzyme was determined

19   using the Bio-Rad Protein Assay (Bio-Rad Laboratories), with bovine serum albumin as

20   the standard. The molar extinction coefficient of 6220 $M^{-1}cm^{-1}$ at 340 nm for both

21   substrates was used to calculate the specific activity, which was expressed as nmole min^{-1}

22   (mg protein)$^{-1}$. The aerobic respiratory chain of *E. coli* contains two types of terminal

23   oxidases, cytochrome bo_3 oxidase and cytochrome bd oxidase. The bo_3-type oxidase is

1 more efficient ($2H^+/e^-$) than the *bd*-type oxidase ($1H^+/e^-$) in creating the electrochemical

2 gradient of protons. The activities of these oxidases cannot be measured separately, so the

3 total activity was measured as ubiquinol-2 (Q_2H_2) oxidase activity. The crude enzyme for

4 the assay of Q_2H_2 oxidase activity was prepared in the same manner as described for the

5 NDHs, except that DTT and glycerol were omitted from the buffer used for cell washing

6 and disruption. The measurement was conducted with 30 μM Q_2H_2 in 50 mM potassium

7 phosphate buffer (pH 7.5) containing 0.1% Tween 20. The absorbance increase at 275 nm

8 was monitored after the enzyme was added to start the reaction. The protein concentration

9 of the crude enzyme was measured by the modified Lowry method with bovine serum

10 albumin as the standard (12). The molar extinction coefficient of 12,250 $M^{-1}cm^{-1}$ at 275

11 nm was used to calculate the specific activity, which was expressed in nmole min^{-1} (mg

12 protein)$^{-1}$.

13 **Immunoblot analysis of the terminal oxidases.** Immunoblot analysis was

14 conducted to investigate the abundance of each of the terminal oxidases. The membrane

15 preparations used for the Q_2H_2 oxidase assay were subjected to SDS-polyacrylamide gel

16 electrophoresis (SDS-PAGE; 23 μg protein per lane). After electrophoresis, the protein

17 bands in the gel were transferred electrophoretically onto a polyvinylidene fluoride

18 (PVDF) membrane (Millipore Corporation, Billerica, MA, USA) at 100 mA for 4 h. After

19 blocking with 3% gelatin and washing, the membrane was incubated for 2 h with

20 anti-cytochrome *bo₃* or anti-cytochrome *bd* antibody. After incubated for 2 h with Protein

21 A-peroxidase, the protein bands were visualized by the addition of color reagents and

22 H_2O_2. Prestained marker proteins (Bio-Rad Laboratories) were used to estimate the

23 relative molecular weights. Anti-cytochrome *bo₃* serum was obtained against the

1   cytochrome bo_3 purified from *E. coli* (Matsushita, K., unpublished) and was used at a

2   50-fold dilution. Dr. Tatsushi Mogi (ATP System Project, ERATO, JST) kindly supplied

3   the anti-cytochrome *bd* serum. The following pretreatment was carried out before use: the

4   anti-cytochrome *bd* serum (0.1 ml) was mixed with 1 ml (~10 mg/ml) of the membranes

5   suspension prepared from *E. coli* GO103 (*ΔcydAB'*) (30) and then incubated at 30°C for 2

6   h. The mixture was centrifuged at 10,000 x *g* for 10 min to obtain the supernatant, which

7   was used as the antibody after a 20-fold dilution.

8

9   **RESULTS**

10

11   **Enhanced glucose metabolism in an F_1-ATPase-defective mutant HBA-1,**

12   **as revealed by chemostat cultures.** To evaluate the effects of an F_1-ATPase defect on

13   glucose metabolism, the mutant HBA-1 and its parent W1485 were cultured in M9

14   minimal medium in a glucose-limited chemostat at the same growth rate ($D = 0.2 \, h^{-1}$), and

15   the fermentation parameters of both strains were calculated. As shown in Table 1, the

16   mutant exhibited reduced biomass production (60%), with increased specific rates of both

17   glucose consumption (168%) and respiration (171%), compared with the parent. Analysis

18   of the fermentation products revealed a substantial excretion of acetate by the mutant,

19   whereas no acetate excretion was observed for the parent. These results clearly

20   demonstrated that glucose metabolism by the F_1-ATPase-defective mutant was enhanced,

21   in agreement with previous observations in different *atp* mutants (21, 40).

22   **Flux analysis.** Based on the observed fermentation parameters (Table 1), the

23   metabolic fluxes within the central metabolic pathways were estimated by a

1   stoichiometric approach. As shown in Fig. 1, the glycolytic flux distribution in HBA-1

2   appeared to be approximately twice that in W1485. However, its distribution in the TCA

3   cycle was only 18% higher in the mutant than in the parent. This difference was due to the

4   acetate excretion observed for HBA-1, whereby the increased flux within the glycolytic

5   pathway overflows, thereby reducing the flow of acetyl-CoA entering the TCA cycle.

6   Increased flow of carbon through glycolytic pathway and in TCA cycle and increased

7   excretion of acetate were also observed in a different *atp* mutant growing in glucose

8   minimal medium under batch culture conditions (21).

9   **Transcriptome analysis.** To determine whether these alterations in glucose

10   metabolism were accompanied by alterations in gene expression, a DNA array analysis

11   was conducted to compare the genomic expression profiles of the parent and mutant. In

12   general, the differences in the expression levels of most genes appeared to be relatively

13   small (less than two-fold) and not statistically significant. Moreover, when differences

14   were detected, most of the genes showed decreased expression levels in the mutant. The

15   similar tendency was observed in the DNA array analysis using cells cultured at a 50%

16   higher dilution rate (D = 0.3 h^{-1}; data not shown). The results are summarized in Table 2,

17   which lists only the genes of known function and relevance and shows the different

18   expression levels in the two strains. Most striking is the absence of the genes involved in

19   glycolysis, despite the enhanced glucose metabolism in the mutant. In contrast, the

20   expression levels of several genes (*gltA*, *icdA, sucA, sucB*, *sucD*, and *mdh*) coding for

21   enzymes in the TCA cycle were significantly decreased, to about 50% of the parental

22   levels. Of these, the decreased expression of *gltA* (44% of the parental level), which codes

23   for citrate synthase, appears to be important in the downregulation of the flux entering

1   into the TCA cycle. Also *aceE* and *aceF* (126% of the parental level), which code for

2   enzymes of the PDH complex, showed a tendency to upregulate. We consider these

3   changes, in combination with reduced expression of *gltA*, to favor the redirection of the

4   glycolytic flux into acetate formation in the mutant (Table 1, Fig. 1). Moreover, the

5   expression of the genes coding for the glyoxylate-shunt enzymes *aceA* and *aceB* were

6   significantly decreased in the mutant (about 60% of the parental level). However, the

7   most interesting finding involves the elevated expression of some genes coding for

8   respiratory chain enzymes. Although the differences were not as prominent, the

9   expression of *ndh*, coding for NDH-2, and *cydA*, coding for cytochrome *bd* oxidase

10   subunit I, were elevated to about 130% of the parental levels. The *cyoA* expression also

11   showed a tendency toward upregulation, but this was not statistically significant. These

12   data suggest that increased respiration in the mutant may be accompanied by alterations

13   in the composition of the respiratory enzymes, which are regulated at the transcription

14   level. In addition to the genes involved in central metabolism, several genes coding for

15   flagella formation and cellular structures (*ompF*) appeared to be significantly repressed.

16   The expression levels of *flhC* and *flhD*, which code for a flagella transcriptional activator,

17   were about 45% below those of the parent, and other flagellar genes (*fliC*, *fliD, flgB, flgC,*

18   and *flgL*) were also repressed. Among the regulatory function genes, only *hns*, coding for

19   the histone-like protein H-NS, was repressed in the mutant (~50%). Given that H-NS is

20   an abundant DNA-binding protein involved in numerous cellular processes, including the

21   replication, recombination, and transcriptional regulation of a large number of genes, a

22   decrease in H-NS protein may have profound effects on *E. coli* cell physiology (33).

23   Besides genes listed in Table 2, the following genes were worth to be referred to as

1 significantly downregulated ones in the mutant (~50%) with known function but with

2 apparently less physiological relevance in response to bioenergetic stress: *hupA* and *hupB*

3 (DNA-binding protein HU), *topA* (DNA topoisomerase I, omega protein I), *grpE* (heat

4 shock protein GrpE), *htpG* (heat shock protein HtpG), *mopB* (GroES protein), *cspD* (cold

5 shock-like protein CspD).

6 To verify the results of the DNA array analysis (Table 2), the expression of four

7 selected genes was monitored by either real-time PCR assay (*ndh*, *cyoA*, and *cydA*) or

8 Northern blot analysis (*hns*). The results, summarized in Table 3, showed comparable

9 tendencies between the DNA array experiments and the real-time PCR assay or Northern

10 blot analysis. Although we did not monitor all the genes listed in Table 2, these results

11 illustrate the reliability of the DNA array experiments for screening and locating

12 important changes in the mutant at the level of transcription.

13 **Enzyme activity in central carbon metabolism**. Based on the results of the

14 fermentation analysis (Table 1, Fig. 1) and the determination of the genomic expression

15 profile (Table 2), several enzymes important to central carbon metabolism were measured

16 to substantiate the observed metabolic changes, especially acetate production, in the

17 mutant (Table 4). In the mutant, the activity of the PDH complex, a key enzyme complex

18 in supplying acetyl-CoA, was twice that in the parent, whereas the activities of three TCA

19 cycle enzymes (citrate synthase, succinyl-CoA synthetase, and malate dehydrogenase) in

20 the mutant appeared to be about half those in the parent. These results agree well with the

21 results obtained in the transcriptome analysis (Table 2), thereby providing validation at

22 the level of enzyme activity. For further insight into the mechanism of acetate production

23 in the mutant, we measured acetate kinase activity, although the transcriptome analysis

1 (Table 2) detected no difference in this enzyme. However, as shown in Table 4, the acetate

2 kinase activity in the mutant was 155% that in the parent. Thus, acetate production in the

3 mutant appears to be triggered by increased acetyl-CoA accumulation attributable to the

4 elevated activity of the PDH complex and the reduced activity of TCA cycle enzymes,

5 especially citrate synthase. The accumulated acetyl-CoA is then readily metabolized into

6 acetate through the acetate kinase-phosphotransacetylase pathway, in which acetate

7 kinase activity is elevated.

8   **Total activities of NDHs and terminal oxidases.** The enhanced rate of

9 respiration (Table 1) as well as the transcriptional upregulation of *ndh* and *cydA* (Tables 2

10 and 3) observed in the mutant led us to measure the total activity of NDHs and terminal

11 oxidases. Two types of NDHs are known in the *E. coli* respiratory chain, NDH-1 and

12 NDH-2 (25). NDH-1 couples the oxidation of NADH to the creation of the

13 electrochemical gradient of protons, whereas NDH-2 does not. Thus, NDH-1 is primarily

14 important for energy recovery from NADH oxidation, and NDH-2 is thought to work as a

15 bypass to modulate electron flow in response to the growth environment. As shown in Fig.

16 2A, the total activity of the NDHs (NDH-1 + NDH-2) was increased 2.3-fold in the

17 mutant compared with the parent. The mutant also showed a 1.8-fold increase in the total

18 activity of the terminal oxidases (cytochrome bo_3 oxidase + cytochrome bd oxidase; Fig.

19 2B). These changes in respiratory enzyme activity correspond to the increased respiration

20 rate in the mutant (1.7-fold; Table 1).

21   **Analysis of the proportions of the NDHs.** The proportion of each NDH

22 isozyme in the mutant (Fig. 2A) was particularly striking. In the parent, total NDH

23 activity was composed of about 60% NDH-1 and 40% NDH-2. However, the NDH-2

1 activity in the mutant was dramatically elevated to 3.7-fold that in the parent, whereas

2 only a slight increase (1.3-fold) was detected in the NDH-1 activity. Therefore, we

3 concluded that the increased total activity of the NDHs was attained primarily through the

4 preferential increase of NDH-2 activity in the mutant, which concurs with the observed

5 upregulation of *ndh* transcription in the mutant (Tables 2 and 3). Consequently, NDH-2

6 activity is predominant in the mutant, comprising up to about 70% of total NDH activity,

7 in contrast to about 40% in the parent.

8   **Analysis of the proportions of the terminal oxidases.** The increased total

9 activity of the terminal oxidases in the mutant (Fig. 2B) prompted us to analyze in detail a

10 possible alteration in the proportion of the terminal oxidases (cytochrome bo_3 oxidase +

11 cytochrome *bd* oxidase). Thus, we have conducted an immunoblot analysis for the

12 terminal oxidases to gain insight into the cytochrome components of the membrane (Fig.

13 3). The band corresponding to subunit I of the *bd*-type oxidase was more abundant in the

14 membrane of the mutant (lane 1) than of the parent (lane 2), whereas the bands for

15 subunits I and II of the *bo*-type oxidase in the membranes did not differ much between the

16 mutant (lane 3) and parent (lane 4). These results correspond to the transcriptional

17 upregulation observed for *cydA* in the mutant (Tables 2 and 3) and indicate an increase in

18 the concentration of the *bd*-type oxidase relative to the *bo*-type oxidase in the mutant.

19

20 **DISCUSSION**

21

22   This study illustrated the overall alterations in an *E. coli* K-12 cell that are

23 associated with defective oxidative phosphorylation due to a mutation in the F_1-ATPase.

1 The results appear to explain how metabolic changes leading to enhanced glucose

2 consumption are possible in response to energy shortages caused by the F_1-ATPase

3 defect.

4   The use of a glucose-limited chemostat for culturing the F_1-ATPase-defective

5 mutant and its parent enabled a precise characterization of both strains growing

6 exponentially at the same rate (D = 0.2 h^{-1}). The enhanced glucose metabolism in the

7 mutant, as revealed by the fermentation parameters (Table 1), was further substantiated

8 by flux analysis (Fig. 1). We calculated twice as much flux through the glycolytic

9 pathway in the mutant. However, we obtained no evidence from the DNA array analysis

10 to suggest the transcriptional upregulation of genes involved in glycolysis (Table 2). Thus,

11 we suggest that the enhanced glycolytic flux was brought about by the allosteric

12 activation of the key enzymes of this pathway, phosphofructokinase I (activation by

13 ADP) (2) and pyruvate kinase II (activation by AMP) (21), under the reduced

14 [ATP]/[ADP] ratio. Interestingly, in the mutant, the flux through the TCA cycle was only

15 18% higher than that in the parent, owing to a redirection of the flux into acetate (Fig. 1),

16 which suggests a stringent metabolic regulation to prevent the flow of the glycolytic

17 pathway from entering the TCA cycle. Results from the enzymatic activities (Table 4)

18 revealed increased activities of the PDH complex and acetate kinase and decreased

19 activities of several TCA cycle enzymes, including citrate synthase. The flux of the TCA

20 cycle in *E. coli* has been shown to be controlled by citrate synthase through feedback

21 inhibition by NADH as a negative effector (37). As the rate of NADH formation in the

22 mutant with enhanced glucose metabolism would be higher than that in the parent, this

23 inhibition, together with the observed alterations in the enzyme activities of the PDH

1   complex, citrate synthase, and acetate kinase, might direct the glycolytic flux into acetate.

2   From an energetic point of view, the number of ATPs generated by substrate-level

3   phosphorylation from either the metabolism of acetyl-CoA through the TCA cycle (ATP

4   generation at the succinyl-CoA synthetase reaction) or the acetate pathway (generation at

5   the acetate kinase reaction) is the same (Fig. 1). Therefore, the physiological importance

6   of the redirection of the glycolytic flux into acetate is not thought to be related to

7   substrate-level phosphorylation in the acetate pathway, but rather to result from a

8   different aspect. The best explanation is the suppression of additional NADH formation

9   through the TCA cycle, because the F_1-ATPase-defective mutant had already generated

10   excess NADH by enhanced glycolysis. As shown in Table 2, the downregulated genes of

11   the TCA cycle enzymes include three (*icdA*, *sucA*, and *mdh*) coding for dehydrogenases

12   generating NADH. These changes, together with reduced citrate synthase activity, appear

13   to reduce NADH formation by the reduced metabolism of acetyl-CoA through the TCA

14   cycle. Furthermore, the downregulation of genes (*aceA*, *aceB*) coding for enzymes in the

15   glyoxylate shunt was also demonstrated (Table 2), which could also reduce NADH

16   formation through malate dehydrogenase, while saving acetyl-CoA for substrate-level

17   phosphorylation coupled with acetate formation (acetate kinase) or the TCA cycle

18   (succinyl-CoA synthetase).

19   In this study, we showed that both the reduction of flow in the TCA cycle and

20   the alteration of respiratory chain components to increase the respiration rate are

21   necessary for the F_1-ATPase-defective mutant to achieve enhanced glucose metabolism.

22   As shown in Figs. 2A and 3, preferential increases in NDH-2 activity and cytochrome *bd*

23   oxidase content were discovered in the respiratory chain of the F_1-ATPase-defective

1   mutant. As components of the respiratory chain of *E. coli*, each NDH and terminal

2   oxidase isozyme exhibits a different efficiency in generating the electrochemical gradient

3   of protons coupled with electron transfer (5, 14): NDH-1 ($2H^+/e^-$) and NDH-2 ($0H^+/e^-$);

4   *bo*-type oxidase ($2H^+/e^-$), and *bd*-type oxidase ($1H^+/e^-$). The increased components of the

5   respiratory chain are bioenergetically less effective, and the net result is that the mutant

6   can recycle the excess NADH formed in its enhanced central metabolism, thus avoiding

7   the generation of excess proton-motive force. In fact, a 20% higher membrane potential

8   has been measured in the *atp*-deletion mutant (21). Therefore, this alteration in the

9   respiratory components seems beneficial from a bioenergetics point of view for enabling

10   the mutant to maintain homeostasis. The observed alterations in the respiratory chain

11   components are a novel finding of an adaptive response in the F_1-ATPase-defective

12   mutant (probably common to all *atp* mutants), and this is in accord with the

13   aforementioned metabolic redirection strategy that limits NADH formation in the TCA

14   cycle. Another interesting aspect was the mechanism for the transcriptional upregulation

15   of NDH-2 and *bd*-type oxidase in response to the *atp* mutation (Tables 2 and 3). Under

16   anaerobic conditions, the expression of *ndh*, which codes for NDH-2, is subject to

17   repression by Fnr, the *fnr* (fumarate nitrate reduction) gene product (17). Under aerobic

18   conditions, Fis (the *fis* gene product; a factor for inversion stimulation) exhibits a growth

19   phase-dependent modulation of transcription from the *ndh* promoter. In the early

20   logarithmic growth phase, when Fis expression is maximal, *ndh* expression is repressed

21   by Fis, thus ensuring that energetically efficient NDH-1 is used. This repression is

22   relieved at the stationary phase, when Fis expression decreases. Thus, NDH-2 seems to be

23   fully expressed when cellular energy is sufficient (16). In this context, the mechanism of

1   the transcriptional upregulation of *ndh* in the F_1-ATPase-defective mutant is difficult to

2   interpret and needs to be clarified in future work. On the other hand, the *cydAB* operon,

3   coding for the *bd*-type oxidase, has been shown to be regulated by the interplay of three

4   global regulatory proteins, Fnr, ArcA (aerobic respiration control; *arcA* gene product),

5   and H-NS, in such a way that its expression is maximal under microaerobic conditions

6   (11, 15, 19, 20). This is physiologically important because the *bd*-type oxidase has a high

7   affinity for oxygen, thereby working effectively under microaerobic conditions. Under

8   aerobic conditions, however, the expression of the *cydAB* operon is normally regulated at

9   a low level because of repression by H-NS (15). In the F_1-ATPase-defective mutant,

10 *bd*-type oxidase content increased even under aerobic conditions (Fig. 3). Interestingly, in

11 the mutant, the expression of H-NS appeared to be repressed to half that of the parent

12 (Tables 2 and 3). Thus, it seems reasonable to attribute the increase of *bd*-type oxidase

13 content to the decrease of H-NS protein.

14   The transcription of seven genes involved in flagellar biogenesis and *ompF*

15 coding for porin was found to be downregulated in the mutant (Table 2). The genes *flhC*

16 and *flhD* constitute the master operon the expression of which switches on the expression

17 of all the other genes involved in flagellar biogenesis (10). As *flhC* and *flhD* are

18 downregulated to less than half in the mutant (Table 2), the expression of the other genes

19 (*flgB, flgC, flgL, fliC* and *fliD*) seems to be affected accordingly. Once again, a decreased

20 expression of *hns* is implicated in these phenomena, because H-NS has been

21 demonstrated to be the positive transcriptional regulator of the *flhDC* operon in vivo (35),

22 and the *hns* mutation has been shown to cause a loss of motility due to the lack of flagella

23 (3). The advantages of these responses are not clear. However, the reduced synthesis of

1 such a large multi-component apparatus (flagellum) and one of the most abundant

2 proteins in *E. coli* in terms of mass (porin) may contribute to cost-savings in biosynthesis

3 (24, 28), especially in an *atp* mutant, in which the ATP supply is limited.

4   In this study, we clarified a series of physiological changes associated with an

5 F_1-ATPase-defective mutation in *E. coli*. The mutation produced not only alterations in

6 central carbon metabolism but also changes in respiratory chain and cellular structure

7 components. The overall results illustrate a novel, yet reasonable, strategy enabling *E.*

8 *coli* to survive energetically difficult conditions brought about by impaired oxidative

9 phosphorylation. Although experimental evidence is lacking, the observed qualitative

10 changes in the mutant, especially the downregulation of TCA cycle enzymes and the

11 upregulation of cytochrome *bd* oxidase, are associated with the operation of the global

12 control network(s), such as the Arc two-component system. The possibility of the

13 involvement of some global control network in the adaptive response of the *atp* mutant

14 and the identification of the signal that is sensed by the network(s) remain to be

15 elucidated.

16

17 **Acknowledgments**

18

04A07004 to M. W.) from the New Energy and Industrial Technology Development Organization (NEDO) of Japan.

References

1. **Aoki, R., M. Wada, N. Takesue, K. Tanaka, and A. Yokota.** 2005. Enhanced glutamic acid production by a H^+-ATPase-defective mutant of *Corynebacterium glutamicum*. Biosci. Biotechnol. Biochem. **69**:1466-1472.

2. **Babul, J.** 1978. Phosphofructokinases from *Escherichia coli*: Purification and characterization of the nonallosteric isozyme. J. Biol. Chem. **253:**4350-4355.

3. **Bertin, P., E. Terao, E. H. Lee, P. Lejeune, C. Colson, A. Danchin, and E. Collatz.** 1994. The H-NS protein is involved in the biogenesis of flagella in *Escherichia coli*. J. Bacteriol. **176**:5537-5540.

4. **Butlin, J. D., G. B. Cox, and F. Gibson.** 1971. Oxidative phosphorylation in *Escherichia coli* K12. Biochem. J. **124**:75-81.

5. **Bogachev, A. V., R. A. Murtazina, and V. P. Skulachev.** 1996. H^+/e^- stoichiometry for NADH dehydrogenase I and dimethyl sulfoxide reductase in anaerobically grown *Escherichia coli* cells. J. Bacteriol. **178**:6233-6237.

6. **Bragg, P. D., and C. Hou.** 1977. Purification and characterization of the inactive Ca^{2+}, Mg^{2+}-activated adenosine triphosphatase of the *unc* A$^-$ mutant *Escherichia coli* AN120. Arch. Biochem. Biophys. **178**:486-494.

7. **Bridger, W. A., R. F. Ramaley, and P. D. Boyer.** 1969. Succinyl Coenzyme A synthetase from *Escherichia coli*. Methods Enzymol. **13**:70-75.

1   8.   **Causey, T. B., K. T. Shanmugam, L. P. Yomano, and L. O. Ingram.** 2004.

2   Engineering *Escherichia coli* for efficient conversion of glucose to pyruvate. Proc.

3   Natl. Acad. Sci. USA. **101**:2235-2240.

4   9.   **Causey, T. B., S. Zhou, K. T. Shanmugam, and L. O. Ingram.** 2003**.**

5   Engineering the metabolism of *Escherichia coli* W3110 for the conversion of sugar

6   to redox-neutral and oxidized products: Homoacetate production. Proc. Natl. Acad.

7   Sci. USA. **100**:825-832.

8 10. **Chilcott, G. S., and K. T. Hughes.** 2000. Coupling of flagellar gene expression to

9   flagellar assembly in *Salmonella enterica* serovar Typhimurium and *Escherichia*

10   *coli.* Microbiol. Mol. Biol. Rev. **64**:694-708.

11 11. **Cotter, P. A., S. B. Melville, J. A. Albrecht, and R. P. Gunsalus.** 1997. Aerobic

12   regulation of cytochrome *d* oxidase (*cydAB*) operon expression in *Escherichia coli*:

13   roles of Fnr and ArcA in repression and activation. Mol. Microbiol. **25**:605-615.

14 12. **Dulley, J. R., and P. A. Grieve.** 1975. A simple technique for eliminating

15   interference by detergents in the Lowry method of protein determination. Anal.

16   Biochem. **64:**136-141.

17 13. **Dunn, S. D.** 1978. Identification of the altered subunit in the inactive F_1ATPase of

18   an *Escherichia coli uncA* mutant. Biochem. Biophys. Res. Commun. **82**:596-602.

19 14. **Gennis, R. B., and V. Stewart.** 1996. Respiration, p. 217-261. *In* F. C. Neidhardt,

20   R. Curtiss III, J. L. Ingraham, E. C. C. Lin, K. B. Low, B. Magasanik, W. S.

21   Reznikoff, M. Riley, M. Schaechter, and H. E. Umbarger (ed.), *Escherichia coli* and

22   *Salmonella*: cellular and molecular biology, 2nd ed. ASM Press, Washington, D. C.

23 15. **Govantes, F., A. V. Orjalo, and R. P. Gunsalus.** 2000. Interplay between three

global regulatory proteins mediates oxygen regulation of the *Escherichia coli* cytochrome *d* oxidase (*cydAB*) operon. Mol. Microbiol. **38**:1061-1073.

16. **Green, J., M. F. Anjum, and J. R. Guest.** 1996. The *ndh*-binding protein (Nbp) regulates the *ndh* gene of *Escherichia coli* in response to growth phase and is identical to Fis. Mol. Microbiol. **20**:1043-1055.

17. **Green, J., and J. R. Guest.** 1994. Regulation of transcription at the *ndh* promoter of *Escherichia coli* by FNR and novel factors. Mol. Microbiol. **12**:433-444.

18. **Holms, H.** 1996. Flux analysis and control of the central metabolic pathways in *Escherichia coli*. FEMS Microbiol. Rev. **19:**85-116.

19. **Fu, H.-A., S. Iuchi, and E. C. C. Lin.** 1991. The requirement of ArcA and Fnr for peak expression of the *cyd* operon in *Escherichia coli* under microaerobic conditions. Mol. Gen. Genet. **226**:209-213.

20. **Iuchi, S., V. Chepuri, H.-A. Fu, R. B. Gennis, and E. C. C. Lin.** 1990. Requirement for terminal cytochromes in generation of the aerobic signal for the *arc* regulatory system in *Escherichia coli*: Study utilizing deletions and *lac* fusions of *cyo* and *cyd*. J. Bacteriol. **172**:6020-6025.

21. **Jensen, P. R., and O. Michelsen.** 1992. Carbon and energy metabolism of *atp* mutants of *Escherichia coli*. J. Bacteriol. **174**:7635-7641.

22. **Koebmann, B. J., H. V. Westerhoff, J. L. Snoep, D. Nilsson, and P. R. Jensen.** 2002. The glycolytic flux in *Escherichia coli* is controlled by the demand for ATP. J. Bacteriol. **184:**3909-3916.

23. **Kotlarz, D., H. Garreau, and H. Buc.** 1975. Regulation of the amount and of the activity of phosphofructokinases and pyruvate kinases in *Escherichia coli*. Biochim.

Biophys. Acta **381:**257-268.

24. **Macnab, R. M.** 1996. Flagella and motility, p. 123-145. *In* F. C. Neidhardt, R. Curtiss III, J. L. Ingraham, E. C. C. Lin, K. B. Low, B. Magasanik, W. S. Reznikoff, M. Riley, M. Schaechter, and H. E. Umbarger (ed.), *Escherichia coli* and *Salmonella*: cellular and molecular biology, 2nd ed. ASM Press, Washington, D. C.

25. **Matsushita, K., T., Ohnishi, and H. R. Kaback.** 1987. NADH-ubiquinone oxidoreductases of the *Escherichia coli* aerobic respiratory chain. Biochemistry **26:** 7732-7737.

26. **Murphey, W. H., C. Barnaby, F. J. Lin, and N. O. Kaplan.** 1967. Malate dehydrogenases. II. Purification and properties of *Bacillus subtilis, Bacillus stearothermophilus,* and *Escherichia coli* malate dehydrogenases. J. Biol. Chem. **242:**1548-1559.

27. **Neidhardt, F. C., J. L. Ingraham, and M. Schaechter.** 1990. Physiology of the bacterial cell: A molecular approach. p. 133-173. Sinauer Associates, Inc., Sunderland, MA.

28. **Nikaido, H.** 1996. Outer Membrane, p. 29-47. *In* F. C. Neidhardt, R. Curtiss III, J. L. Ingraham, E. C. C. Lin, K. B. Low, B. Magasanik, W. S. Reznikoff, M. Riley, M. Schaechter, and H. E. Umbarger (ed.), *Escherichia coli* and *Salmonella*: cellular and molecular biology, 2nd ed. ASM Press, Washington, D. C.

29. **Noumi T., M. Futai, and H. Kanazawa.** 1984. Replacement of serine 373 by phenylalanine in the α subunit of *Escherichia coli* F_1-ATPase results in loss of steady-state catalysis by the enzyme. J. Biol. Chem. **259:**10076-10079.

30. **Oden, K. L., L. C. DeVeaux, C. R. T. Vibat, J. E. Cronan Jr., and R. B. Gennis.**

1990. Genomic replacement in *Escherichia coli* K-12 using covalently closed

circular plasmid DNA. Gene **96**: 29-36.

31. **Riondet, C., R. Cachon, Y. Waché, G. Alcaraz, and C. Diviès.** 2000. Extracellular oxidoreduction potential modifies carbon and electron flow in *Escherichia coli.* J. Bacteriol. **182**:620-626.

32. **Santana, M., M. S. Ionescu, A. Vertes, R. Longin, F. Kunst, A. Danchin, and P. Glaser.** 1994. *Bacillus subtilis* F_0F_1 ATPase: DNA sequence of the *atp* operon and characterization of *atp* mutants. J. Bacteriol. **176:**6802-6811.

33. **Schoröder, O., and R. Wagner.** 2002. The bacterial regulatory protein H-NS – A versatile modulator of nucleic acid structures. Biol. Chem. **383**:945-960.

34. **Sekine, H., T. Shimada, C. Hayashi, A. Ishiguro, F. Tomita, and A. Yokota.** 2001. H^+-ATPase defect in *Corynebacterium glutamicum* abolishes glutamic acid production with enhancement of glucose consumption rate. Appl. Microbiol. Biotechnol. **57**:534-540.

35. **Soutourina, O., A. Kolb, E. Krin, C. Laurent-Winter, S. Rimsky, A. Danchin, and P. Bertin.** 1999. Multiple control of flagellum biosynthesis in *Escherichia coli*: Role of H-NS protein and the cyclic AMP-catabolite activator protein complex in transcription of the *flhDC* master operon. J. Bacteriol. **181**:7500-7508.

36. **Weitzman, P. D. J.** 1969. Citrate synthase from *Escherichia coli.* Methods Enzymol. **13**:22-26.

37. **Weitzman, P. D. J.** 1981. Unity and diversity in some bacterial citric acid-cycle enzymes. Adv. Microb. Physiol. **22:**185-244.

38. **Yokota, A.**, S, Amachi, and F. Tomita.** 1999. Pyruvate, production using defective

1   ATPase activity, p. 2261-2268. *In* M. C. Flickinger, and S. W. Drew (ed.),

2   Encyclopedia of bioprocess technology: fermentation, biocatalysis, and

3   bioseparation. John Wiley & Sons, Inc., New York, NY.

4 39. **Yokota, A., H. Shimizu, Y. Terasawa, N. Takaoka, and F. Tomita.** 1994. Pyruvic

5   acid production by a lipoic acid auxotroph of *Escherichia coli* W1485. Appl.

6   Microbiol. Biotechnol. **41**:638-643.

7 40. **Yokota, A., Y. Terasawa, N. Takaoka, H. Shimizu, and F. Tomita.** 1994. Pyruvic

8   acid production by an F_1-ATPase-defective mutant of *Escherichia coli* W1485*lip2*.

9   Biosci. Biotechnol. Biochem. **58**:2164-2167.

1   Table 1. Parameters in the chemostat cultures.

2

Strain	Y_{CELL}[a]	Fluxes[b]			Respiration[c]
		Glucose	Acetate	2-OGA	
W1485	0.056 (1)[d]	3.57 (1)	0.00	0.20	14.4 (1)
HBA-1	0.033 (0.6)	6.00 (1.68)	4.30	0.10	24.6 (1.71)

7

8   An F_1-ATPase-defective mutant, HBA-1, and its parent strain, W1485, were cultured

9   under glucose-limited chemostat conditions in M9 minimal medium at a dilution rate of

10   0.2 h^{-1}, as described in Materials and Methods.

11   [a] Y_{CELL}, cell yield in g dry cell/mmol glucose.

12   [b] Fluxes, consumption of glucose or excretion of acetate or 2-oxo-glutarate (2-OGA) in

13   mmol (g dry cell)$^{-1}$ h^{-1}.

14   [c] mmol O_2 h^{-1} (g dry cell)$^{-1}$.

15   [d] Fold difference between strains W1485 and HBA-1.

TABLE 2. Summary of genes showing different expression levels between strains W1485 and HBA-1 grown in glucose-limited chemostat culture, as revealed by DNA array analysis[a].

Gene	Gene product	Averaged spot intensities [b]		Standard deviation		Ratio [c] (HBA-1/ W1485)
		W1485	HBA-1	W1485	HBA-1	
aceE	pyruvate dehydrogenase E1 component	1.18E –04	1.48E –04	2.09E –05	3.27E –05	1.26
aceF	E2 of pyruvate dehydrogenase	1.52E –04	1.92E –04	2.79E –05	3.52E –05	1.26*
gltA	citrate synthase	4.05E –04	1.80E –04	7.80E –05	6.03E –05	0.45*
icdA	isocitrate dehydrogenase	2.95E –04	1.80E –04	4.53E –05	2.27E –05	0.61*
sucA	2-oxoglutalate dehydrogenase E1 component	1.34E –04	7.63E –05	3.45E –05	2.25E –05	0.57*
sucB	dihydrolipoamide succinyltransferase component (E2)	1.29E –04	6.19E –05	2.94E –05	1.52E –05	0.48*
sucD	succinyl-CoA synthetase α chain	4.86E –04	1.72E –04	1.87E –04	8.94E –05	0.35*
mdh	malate dehydrogenase	3.18E –04	1.34E –04	1.14E –04	3.66E –05	0.42*

aceA	isocitrate lyase	2.37E –04	1.52E –04	5.90E –05	3.01E –04	0.64*
aceB	malate synthase A	3.82E –04	2.22E –04	7.72E –05	9.11E –05	0.58*
ndh	NADH dehydrogenase II	8.25E –05	1.09E –04	1.18E –05	1.94E –05	1.32*
nuoA	NADH dehydrogenase I chain A	5.78E –05	4.96E –05	1.27E –05	8.07E –06	0.86
cydA	cytochrome *d* oxidase subunit I	3.00E –04	4.02E –04	1.61E –04	2.43E –04	1.34*
cyoA	cytochrome *o* oxidase subunit II	3.24E –04	4.19E –04	1.51E –04	2.49E –04	1.30
flhC	flagellar transcriptional activator	1.99E –04	8.96E –05	4.14 E–07	8.26E –06	0.45 *
flhD	flagellar transcriptional activator	2.57E –04	1.12E –04	2.68E –07	2.28E –05	0.44*
fliC	flagellin	8.68E –04	3.64E –04	4.55E –05	1.00E –04	0.42*
fliD	flagellar hook-associated protein 2	1.43E –04	8.07E –05	1.68E –05	2.70E –05	0.56*
flgB	putative flagellar basal-body rod protein FlgB	3.19E –04	1.85E –04	1.85E –05	6.18E –05	0.58*
flgC	putative flagellar basal-body rod protein FlgC	1.52E –04	8.88E –05	6.24E –06	2.77E –05	0.58*
flgL	flagellar hook-associated protein 3	2.18E –04	1.20E –04	9.01E –06	1.79E –05	0.55*
ompF	outer membrane protein F precursor	2.58E –03	1.21E –03	5.83E –04	3.00E –04	0.47*

nmpC	outer membrane porin protein NmpC precursor	1.60E –04	1.10E –04	5.19E –05	1.84E –05	0.69*
hns	histone-like protein H-NS	1.20E –04	6.06E –04	3.18E –04	3.57E –04	0.50*

[a] The results are from eight independent DNA array analyses.

[b] Expressed as the percentage of the total intensity of all the spots on the DNA array.

[c] Expression ratio of HBA-1 to W1485. The asterisk indicates significant t-test differences ($p < 0.05$).

Table 3. Comparison of the expression ratios of several genes, as determined by DNA

array and Northern blot analysis or real-time PCR analysis.

Gene	Expression ratio (HBA-1/W1485)		
	DNA array[a]	Northern blot[c]	Real-time PCR[c]
ndh	1.32*	ND[b]	2.40
cyoA	1.30	ND	1.67
cydA	1.34*	ND	1.38
hns	0.50*	0.67	ND

[a] Adapted from Table 1. The asterisk indicates significant t-test differences ($p < 0.05$).

[b] Not determined.

[c] The assays were repeated two to three times.

Table 4. Activity of several central carbon metabolism enzymes.

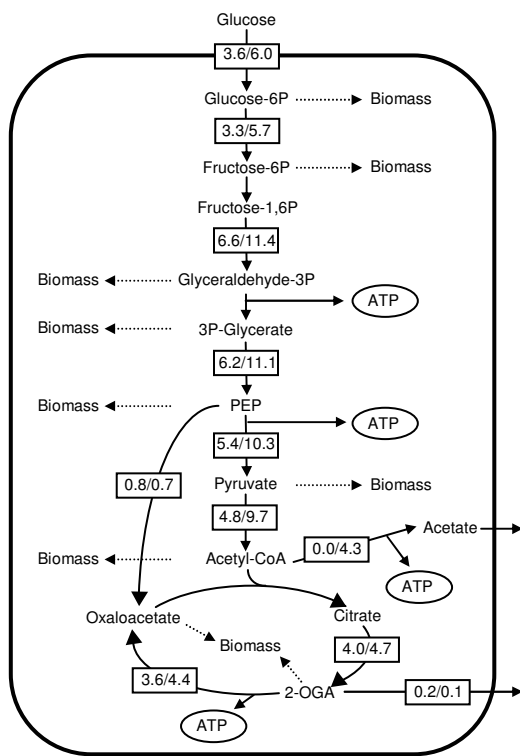| Enzyme	Specific activity [a] (nmol/min/mg)		Ratio (HBA-1/ W1485)
	W1485	HBA-1	
PDH complex	74	152	2.05
Acetate kinase	2532	3933	1.55
Citrate synthase	597	375	0.63
Succinyl-CoA synthetase	384	217	0.57
Malate dehydrogenase	13064	6039	0.46

[a] Average values from at least two independent experiments.

(Figure legends)

Fig. 1. Flux analysis in the central metabolic pathways of the parent and mutant. The values in the boxes show the flux of the parent, W1485 (left), and the mutant, HBA-1 (right), in mmol (g dry cell)$^{-1}$ h^{-1}.

Fig. 2. Analysis of respiratory chain components based on enzyme activity measurements, expressed as nmol min^{-1} (mg protein)$^{-1}$. (A) NDH-1 activity: W1485, 267 ± 125 (n = 10); HBA-1, 338 ± 110 (n = 8). NDH-2 activity: W1485, 197 ± 87 (n = 10); HBA-1, 723 ± 112 (n = 8). (B) Q$_2$H$_2$ oxidase activity: W1485, 1400 ± 14 (n = 2); HBA-1, 2460 ± 594 (n = 2).

Fig. 3. Immunoblot analysis of terminal oxidases. After SDS polyacrylamide gel electrophoresis of the membrane preparations of the parent and mutant, the protein bands were transferred to PVDF membranes, and then probed with anti-cytochrome *bo*$_3$ serum (*bo*) or anti-cytochrome *bd* serum (*bd*). Lanes 1 and 3, HBA-1; Lanes 2 and 4, W1485; M, marker proteins. The data shown are representative of at least three independent experiments that gave similar results.

Glucose

3.6/6.0

Glucose-6P ·············▶ Biomass

3.3/5.7

Fructose-6P ·············▶ Biomass

Fructose-1,6P

6.6/11.4

Biomass ◀············· Glyceraldehyde-3P ────▶ (ATP)

Biomass ◀············· 3P-Glycerate

6.2/11.1

Biomass ◀············· PEP ────▶ (ATP)

5.4/10.3

0.8/0.7

Pyruvate ·············▶ Biomass

4.8/9.7

Acetate ─▶

Biomass ◀············· Acetyl-CoA   0.0/4.3

(ATP)

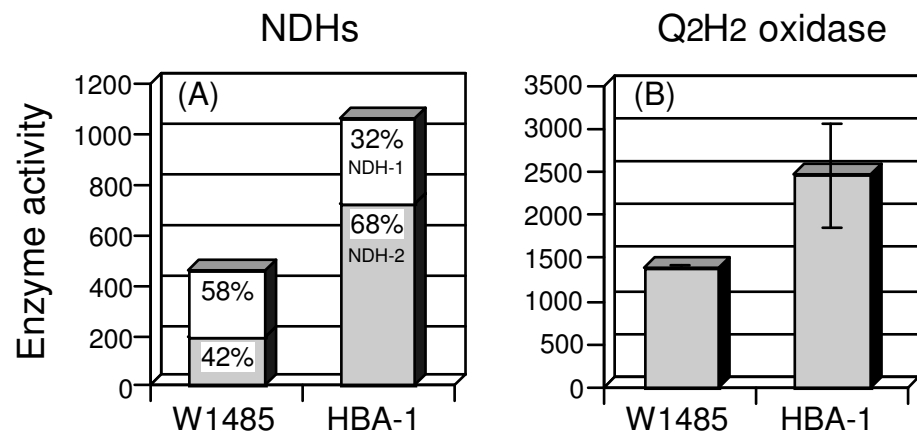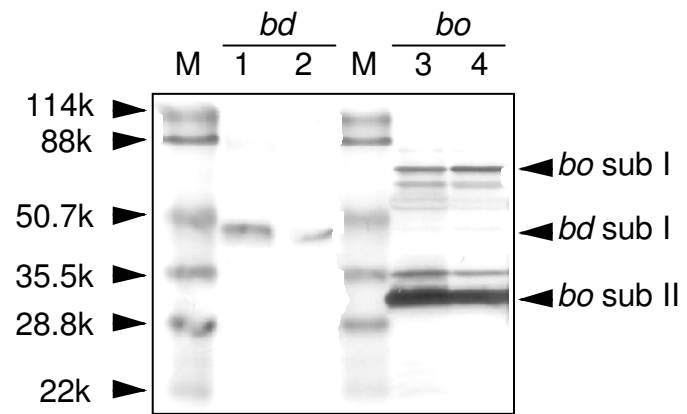Oxaloacetate ······· Biomass   Citrate

4.0/4.7

3.6/4.4   2-OGA   0.2/0.1 ─▶

(ATP)

FIG. 2. Noda et al.

FIG. 3. Noda et al.